J Electr Eng Technol.2018; 13(2): 620-630
http://doi.org/10.5370/JEET.2018.13.2.620

ISSN(Print) 1975-0102
ISSN(Online) 2093-7423

A Positioning Method of Distributed Power System by Considering Characteristics of Droop Control in a DC Microgrid

Byoung-Sun Ko*, Gi-Young Lee*, Sang-Il Kim*, Rae-Young Kim†, Jin-Tae Cho and Ju-Yong Kim****

Abstract – In this paper, a positioning method of distributed power system is proposed to minimize the average voltage variation of a DC microgrid through voltage sensitivity analysis. The voltage sensitivity under a droop control depends on the position of the distributed power system. In order to acquire a precise voltage sensitivity under a droop control, we analyzed the power flow by introducing a droop bus with the considerations of the droop characteristics. The results of the positioning method are verified through PSCAD/EMTDC simulation.

Keywords: DC microgrid, Droop control, Positioning, Power flow analysis, Voltage sensitivity

1. Introduction

The demand for renewable energy sources (RESs) is increasing due to the constant increment in electricity demands and environmental problems such as global warming. Accordingly, microgrids (MGs) for improving the efficiency and reliability of power networks by utilizing renewable energy from RESs have been actively researched [1]. An MG is a small power grid composed of a distributed power system (DPS) such as an RES and an energy storage system (ESS) and various loads. An MG constitutes a bidirectional structure where customers can produce or consume electric power, out of the unidirectional structure of an existing power grid. As a result, MGs can solve problems related to the expansion of electric power facilities and the inconsistencies between production and consumption in an existing power network. In addition, an MG is capable of cooperative or independent operation with the grid, has flexibility in operation, and can improve the reliability of power supply [2-5].

Methods used to control MGs can be divided into a centralized control method and a distributed control method. In the centralized control method, the central controller accumulates local information from the sub-device and calculates the control command. The calculated control command is transferred to the sub-device through a communication network, and the sub-device is operated by the transmitted control command. Because this centralized control method can calculate the optimum energy flow and send the command value to each device, optimized MG operation can be achieved [6]. However, there are still problems such as the large dependency of the communication network and operation interruption caused by the occurrence of single points of failure. To overcome these problems, a distributed control method based on droop control has been studied. Droop control is the most common automatic control strategy that adds a virtual impedance control loop to change the voltage reference; this performs voltage regulation and load sharing simultaneously without a communication network [7]. However, the distributed control method based on droop control also has problems that a large voltage variation and unbalanced load sharing are caused by the line impedance [8].

In addition to research on techniques for MG control, studies have been conducted to optimize the power grid by selecting the optimal locations of various DPSs. In [9, 10], a positioning method that considered the installation cost of DPSs was proposed to optimize the operation cost. [11, 12] proposed a placement method to improve the efficiency of the power grid by analyzing the effects of line losses according to the placement of various devices in the MG. [13] proposed a location method for RESs in interconnected MGs by considering the randomness of power generation and load demand. [14] emphasized the role of ESSs as backup power sources and proposed an ESS positioning method with an intelligent load cutoff plan to minimize the social cost in the case of a power outage. Most of the proposed methods have been studied in the MG networks operated by the centralized control method. Additionally, the DPSs used to maintain the voltage of MG networks have been modeled as slack buses with an ideal voltage source.

However, a DPS operated by droop control has voltage-current characteristics where the output voltage is changed by the virtual impedance control loop. These voltage-current characteristics are affected by the line impedance, and the performance of the voltage regulation and load

† Corresponding Author: Dept. of Electrical and Biomedical Engineering, Hanyang University, Korea. (rykim@hanyang.ac.kr)
* Dept. of Electrical Engineering, Hanyang University, Korea. ({byoungsun1, popple87, si401}@hanyang.ac.kr)
** Korea Electric Power Research Institute(KEPRI), Korea Electric Power Corporation(KEPKO), Daejeon, Korea ({jintae.cho, juyong.kim@kepco.co.kr)
Received: June 27, 2017; Accepted: November 13, 2017

sharing depend on the position of the DPS. Therefore, modelling the DPS with a conventional slack bus diminishes the accuracy of the analysis and, at worst, it can deteriorate the voltage regulation of the grid network.

Although many positioning methods of DPSs have been proposed so far, an appropriate interpretation for this has hardly been studied. Accordingly, a positioning method that considers the characteristics of droop control has not been proposed in particular.

In this paper, a positioning method is proposed to minimize the average voltage variation of an MG applying a distributed control method based on droop control. Power flow analysis is performed to derive the voltage sensitivity, and the location of the DPS is determined based on this analysis. In addition, a droop bus that represents the characteristics of droop control is introduced to enhance the accuracy of the voltage sensitivity analysis. The voltage sensitivity according to the position of the DPS is calculated and compared. Finally, a positioning method of the DPS that can be used to minimize the average voltage variation of the MG is described.

This paper is organized as follows. In Section II, droop control is briefly described and the effects of the line impedance on droop control are analyzed. In Section III, the voltage sensitivity is derived based on the power flow analysis. In Section IV, the proposed positioning method is explained. Finally, Section V verifies the validity of the proposed positioning method though simulation results using PSCAD/EMTDC.

2. Droop control

2.1 Operation principle

Fig. 1 shows the overall block diagram of the DPS operated by droop control. As shown in the figure, the output current i_o is fed back to generate a new voltage reference v^*_o through the virtual impedance R_D; this obtains load sharing that is proportional to the rated capacity. v^*_o and R_D are expressed as (1) and (2) where G_D, ΔV_{nom}, $V_{dc,min}$, V_{nom} and P_{rated} are the virtual admittance, permissible voltage variation, minimum voltage, base

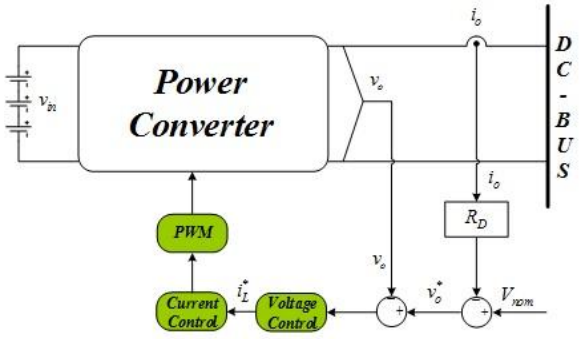

Fig. 1. Block diagram of droop control

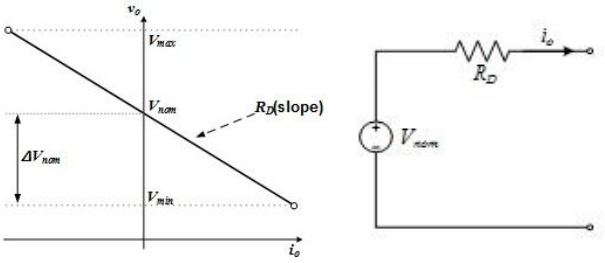

(a) V-I characteristics curve (b) Droop bus model

Fig. 2. Characteristics of droop control

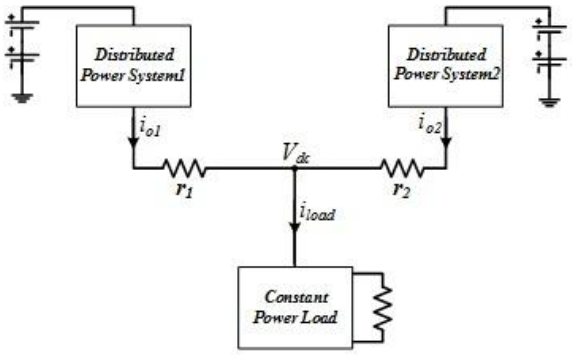

Fig. 3. Simple DC MG

voltage, and rated capacity of the DPS, respectively.

$$v^*_o = V_{nom} - R_D \cdot i_o \tag{1}$$

$$R_D = \frac{1}{G_D} = \frac{\Delta V_{nom} \cdot V_{dc,\min}}{P_{rated}} \tag{2}$$

Fig. 2 shows the voltage-current characteristics of the DPS operated by droop control and the corresponding droop bus model. As can be seen from the voltage-current characteristic curve in fig. 2 (a), the DPS shows the same voltage drop characteristics as the voltage source with internal resistance. Therefore, the DPS controlled by droop control can be expressed with the droop bus model shown in fig. 2 (b).

2.2 Influence of line impedance

Fig. 3 shows a DC MG that includes two DPSs and one load. Assuming that the DPS is driven by droop control and the load consumes a constant amount of power, the equivalent circuit shown in fig. 3 can be expressed as fig. 4 where the load is modeled as a current sink. When the node analysis is executed based on the output of the DPS, the output currents i_{o1}, i_{o2} can be derived as shown in (3). The voltage variation ΔV_{dc} of the DC MG is expressed by (4) where ΔV_{dc} is the magnitude of the voltage variation relative to the base voltage V_{nom} in a situation where power is generated or consumed. R_{D1} and R_{D2} represent the virtual impedance of DPS1 and DPS2, respectively, and r_1 and r_2

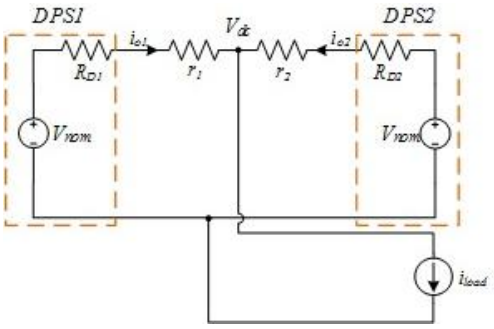

Fig. 4. Equivalent simple DC MG

denote the line impedance.

$$i_{o1} = \frac{R_{D2} + r_2}{R_{D1} + r_1 + R_{D2} + r_2} i_{load} \quad i_{o2} = \frac{R_{D1} + r_1}{R_{D1} + r_1 + R_{D2} + r_2} i_{load} \tag{3}$$

$$\Delta V_{dc} = V_{nom} - V_{dc} = \left(R_{D1} + r_1\right) i_{o1} = \left(R_{D2} + r_2\right) i_{o2} \tag{4}$$

As can be seen from (4), ΔV_{dc} is determined by the output current, virtual impedance, and line impedance. Note that a positive voltage variation means that the DPS generates power. If r_1 and r_2 are small enough to be ignored, ΔV_{dc} is determined only by R_{D1} and R_{D2}. On the contrary, when r_1 and r_2 are relatively large, ΔV_{dc} is affected by them and becomes large under equal power consumption and generation.

3. Power Flow Analysis

Generally, the power flow of the DC MG is analyzed to appropriately select the grid structure, the rated capacity and location of various equipment. Various forms of bus are used to account for the characteristics of the source and load. For example, a slack bus represents an ideal voltage source that always maintains a constant voltage [15, 16].

Fig. 5 shows the power relationship in a typical DC MG. The current I_i and power P_i of bus-i are derived through node analysis as shown in (5) and (6) where V_i and G_{ij} represent the voltage of bus-i and the admittance between bus-i and bus-j, respectively.

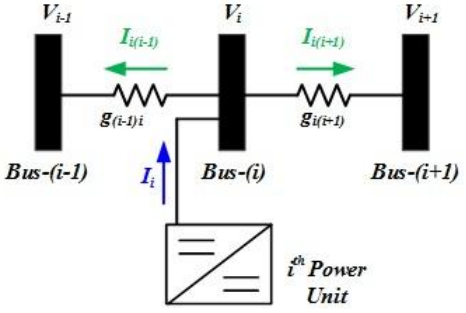

Fig. 5. Power relationship at the DC-network

$$I_i = \sum_{\substack{j=1 \\ j \neq i}}^{n} G_{ij} \left(V_i - V_j\right) \tag{5}$$

$$P_i = V_i I_i = V_i \sum_{\substack{j=1 \\ j \neq i}}^{n} G_{ij} \left(V_i - V_j\right) \tag{6}$$

Eq. (5) and (6) can be normalized and expressed as (7) and (8).

$$i_i = \sum_{\substack{j=1 \\ j \neq i}}^{n} g_{ij} \left(v_i - v_j\right) \tag{7}$$

$$p_i = v_i i_i = v_i \sum_{\substack{j=1 \\ j \neq i}}^{n} g_{ij} \left(v_i - v_j\right) \tag{8}$$

where $v_i = V_i/V_{nom}$, $g_{ij} = G_{ij}/G_{nom}$, $p_i = P_i/P_{nom}$. V_{nom} and P_{nom} are the base voltage and base power, respectively, and $G_{nom} = P_{nom}/V^2_{nom}$.

Using (8), the power of a grid consisting of n-buses can be expressed as (9).

$$p = \begin{bmatrix} p_1 \\ \vdots \\ p_n \end{bmatrix} = \begin{bmatrix} v_1 \sum_{\substack{j=1 \\ j \neq 1}}^{n} g_{1j} \left(v_1 - v_j\right) \\ \vdots \\ v_n \sum_{\substack{j=1 \\ j \neq n}}^{n} g_{nj} \left(v_n - v_j\right) \end{bmatrix}. \tag{9}$$

The Jacobian matrix [J] that is expressed by (11) can be obtained by taking the partial derivatives of (9), as expressed in (10) where Δp and Δv represent the output variation and the voltage variation of the corresponding bus, respectively. The symbol "[ ]" implies a matrix representation.

$$\frac{\partial p}{\partial v_i} = \lim_{h \to 0} \frac{p\left(v_1, \cdots, v_{k-1}, v_k + h, v_{k+1}, \cdots, v_n\right) - p\left(v_1, \cdots, v_k, \cdots, v_n\right)}{h} \tag{10}$$

$$[J] = \frac{\Delta p}{\Delta v} = \begin{bmatrix} \frac{\partial p_1}{\partial v_1} & \frac{\partial p_1}{\partial v_2} & \cdots & \frac{\partial p_1}{\partial v_n} \\ \frac{\partial p_2}{\partial v_1} & \frac{\partial p_2}{\partial v_2} & \cdots & \frac{\partial p_2}{\partial v_n} \\ \vdots & \vdots & \vdots & \vdots \\ \frac{\partial p_n}{\partial v_1} & \frac{\partial p_n}{\partial v_2} & \cdots & \frac{\partial p_n}{\partial v_n} \end{bmatrix} \tag{11}$$

Finally, by taking the inverse matrix of (11), the voltage sensitivity [S], which indicates the voltage variation rate

with respect to the power change of each bus can be derived as (12). Note that this voltage sensitivity [S] anticipates the voltage variation when power variation occurs on any bus, as shown by (13) where a positive voltage variation means that the bus absorbs power.

$$[S]=\frac{\Delta v}{\Delta p}=[J]^{-1} \tag{12}$$

$$\begin{bmatrix}\Delta v_1\\ \Delta v_2\\ \vdots\\ \Delta v_n\end{bmatrix}=\begin{bmatrix}s_{12} & s_{12} & \cdots & s_{1n}\\ s_{21} & s_{22} & \cdots & s_{2n}\\ \vdots & \vdots & \vdots & \vdots\\ s_{n1} & s_{n2} & \cdots & s_{nn}\end{bmatrix}\begin{bmatrix}\Delta p_1\\ \Delta p_2\\ \vdots\\ \Delta p_n\end{bmatrix} \tag{13}$$

3.1 Existing power flow analysis

Fig. 6 shows an example of a DC MG with a 5-bus radial structure. The DC MG consists of an ESS, four loads, and one PV. Table 1 summarizes the ratings and locations of each device. It is assumed that the PV operates as a constant power source by MPPT control, while the ESS is operated by droop control to maintain the DC MG voltage. Fig. 7 shows the equivalent circuit where the ESS that regulates the voltage of the DC MG is modeled by a slack bus, and the PV and loads are modeled by a current source and sink.

By applying (9) to the equivalent circuit shown in fig. 7, the power of the DC MG is derived as (14).

Table 1. Ratings and locations of units

Location	Unit	Rating
Bus-1	ESS	110 kW
Bus-2	PV, Load1	110 kW, 25 kW
Bus-3,4,5	Load2,3,4	25 kW

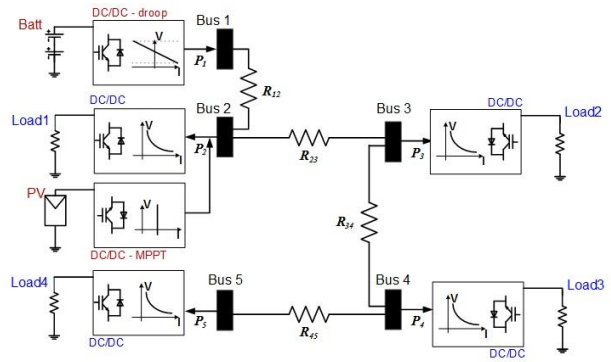

Fig. 6. 5-bus DC MG

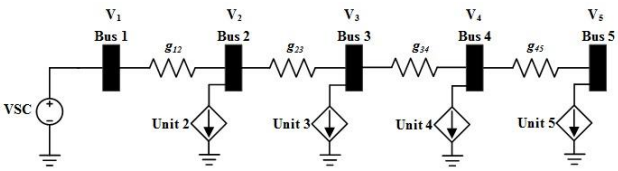

Fig. 7. Equivalent 5-bus DC MG with a slack bus

$$p=\begin{bmatrix}p_2\\ p_3\\ p_4\\ p_5\end{bmatrix}=\begin{bmatrix}g_{12}v_2(v_2-v_1)+g_{23}v_2(v_2-v_3)\\ g_{23}v_3(v_3-v_2)+g_{34}v_3(v_3-v_4)\\ g_{34}v_4(v_4-v_3)+g_{45}v_4(v_4-v_5)\\ g_{45}v_5(v_5-v_4)\end{bmatrix} \tag{14}$$

By taking the partial derivatives of (14), the Jacobian matrix $[J]_{slack}$ is obtained as shown in the Appendix (A-1).

By applying (12) to $[J]_{slack}$, $[S]_{slack}$ is also obtained and expressed as (15). Eq. (15) shows the numerical result when the line constants in Table 2 are used. Note that the initial voltage of bus-i is assumed to be 1 p.u. under the conditions of no load or power generation.

$$[S]_{slack}=[J]_{slack}^{-1}=\begin{bmatrix}0.0293 & 0.0293 & 0.0293 & 0.0293\\ 0.0293 & 0.0587 & 0.0587 & 0.0587\\ 0.0293 & 0.0587 & 0.0807 & 0.0807\\ 0.0293 & 0.0587 & 0.0807 & 0.1027\end{bmatrix} \tag{15}$$

3.2 Power flow analysis using a droop bus

Fig. 8 shows the equivalent circuit where the ESS of the

Table 2. System parameters of the 5-bus DC MG

Symbol	Quantity	Values
V_{nom}	Nominal Voltage	1500 V
P_{nom}	Nominal Power	110 kW
$V_{dc,\min}$	Minimum Voltage	1400 V
ΔV_{nom}	Allowable Voltage Variation	100 V
G_{nom}	Nominal Admittance	0.0489 Ω^{-1}
$G_{D,ESS}$	Virtual Admittance	0.7857 Ω^{-1}
$G_{D,ESS,add}$	Virtual Admittance	0.7857 Ω^{-1}
G_{12}	Line Admittance	1.6667 Ω^{-1}
G_{23}	Line Admittance	1.6667 Ω^{-1}
G_{34}	Line Admittance	2.2222 Ω^{-1}
G_{45}	Line Admittance	2.2222 Ω^{-1}
G_{25}	Line Admittance	2.1084 Ω^{-1}
G_{35}	Line Admittance	1.5713 Ω^{-1}

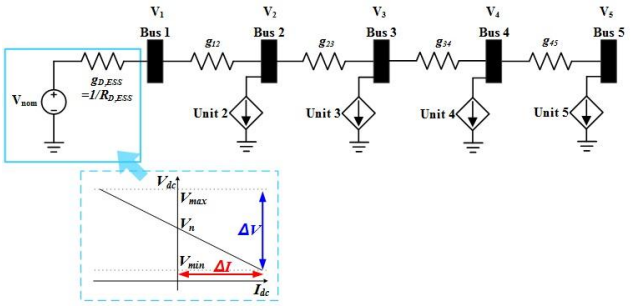

Fig. 8. Equivalent 5-bus DC MG with a droop bus

DC MG is modeled by a droop bus. As similar way earlier explained, by applying (9)-(12) to fig. 8, the power of the DC MG, the Jacobian matrix $[J]_{droop}$, and the voltage sensitivity $[S]_{droop}$ can be obtained as (16), (A-2), and (17), respectively, where $g_{D,ESS}$ is the virtual admittance of the ESS. This is calculated with (2) and is expressed by the p.u.

$$p=\begin{bmatrix} p_1 \\ p_2 \\ p_3 \\ p_4 \\ p_5 \end{bmatrix}=\begin{bmatrix} g_{D,\mathrm{ESS}}v_1\left(v_1-v_{nom}\right)+g_{12}v_1\left(v_1-v_2\right) \\ g_{12}v_2\left(v_2-v_1\right)+g_{23}v_2\left(v_2-v_3\right) \\ g_{23}v_3\left(v_3-v_2\right)+g_{34}v_3\left(v_3-v_4\right) \\ g_{34}v_4\left(v_4-v_3\right)+g_{45}v_4\left(v_4-v_5\right) \\ g_{45}v_5\left(v_5-v_4\right) \end{bmatrix} \quad (16)$$

$$[S]_{droop}=[J]_{droop}^{-1}=\begin{bmatrix} 0.0622 & 0.0622 & 0.0622 & 0.0622 & 0.0622 \\ 0.0622 & 0.0729 & 0.0729 & 0.0729 & 0.0729 \\ 0.0622 & 0.0729 & 0.0836 & 0.0836 & 0.0836 \\ 0.0622 & 0.0729 & 0.0836 & 0.0116 & 0.0116 \\ 0.0622 & 0.0729 & 0.0836 & 0.0116 & 0.1262 \end{bmatrix} \quad (17)$$

Comparing (16) and (A-2) with (14) and (A-1) shows that the term composed of the $g_{D,ESS}$ appears when the ESS is modeled as a droop bus. In other words, it is possible to analyze the power flow more accurately by considering the characteristics of droop control, as compared to the conventional slack bus case.

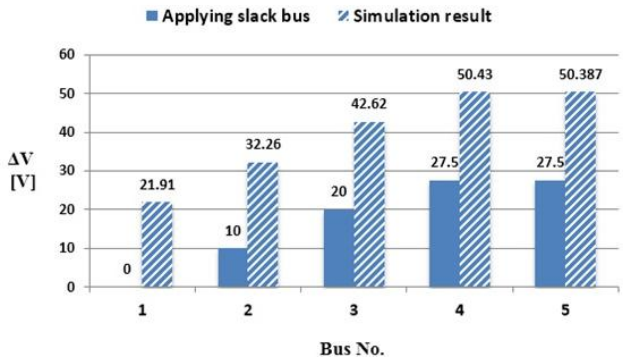

(a) Slack bus case

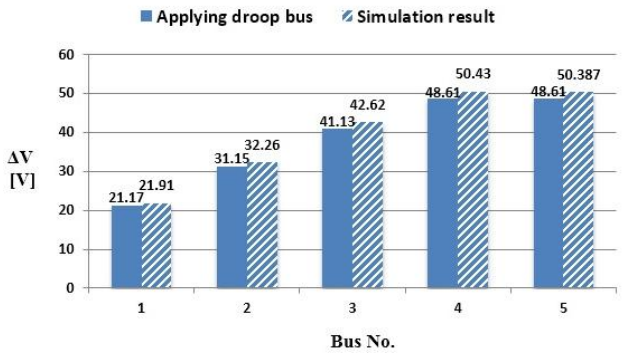

(b) Droop bus case

Fig. 9. Result of power flow analysis

3.3 Improved accuracy with a droop bus

Fig. 9 shows the difference between voltage variations through simulation and voltage sensitivity [S]. In the DC MG shown in Fig. 6, it is simulated that the ESS on the bus-1 operated by droop control and the load on bus-4 increases from 0kW to 25kW. Fig. 9(a) shows the simulation result and voltage variation of each bus calculated through (15). As can be seen from the figure, there is a large error in the analysis result using slack bus, which is about 22V for each bus. Since the ESS that operated by droop control is modeled as slack bus, it does not reflect the characteristics of the droop control and causes the large error. Fig. 9(b) shows the simulation result and voltage variation calculated by (17). In this case, the error is about 2V and relatively accurate. That is, when the distributed control method based on droop control is applied to an MG, applying a droop bus can improve the accuracy of the power flow analysis.

4. Proposed Positioning Method of DPS

The addition of DPS operated by droop control to improve the voltage regulation influences the voltage sensitivity of the DC MG, so it is necessary to ensure the voltage regulation performance by properly positioning the DPS.

For example, as shown in fig. 10, it is assumed that the ESS operated by droop control is additionally placed on bus-3 in the DC MG of fig. 6. By modeling this ESS as a droop bus and applying (9)-(11), the power of the DC MG and the Jacobian matrix $[J]_{\mathrm{droop,bus3}}$ are derived as (18) and (A-3), respectively, where $g_{D,ESS,add}$ is the virtual admittance of the added ESS.

$$p=\begin{bmatrix} p_1 \\ p_2 \\ p_3 \\ p_4 \\ p_5 \end{bmatrix}=\begin{bmatrix} g_{D,\mathrm{ESS}}v_1\left(v_1-v_{nom}\right)+g_{12}v_1\left(v_1-v_2\right) \\ g_{12}v_2\left(v_2-v_1\right)+g_{23}v_2\left(v_2-v_3\right) \\ g_{23}v_3\left(v_3-v_2\right)+g_{34}v_3\left(v_3-v_4\right) \\ +g_{D,ESS,add}v_3\left(v_3-v_{nom}\right) \\ g_{34}v_4\left(v_4-v_3\right)+g_{45}v_4\left(v_4-v_5\right) \\ g_{45}v_5\left(v_5-v_4\right) \end{bmatrix} \quad (18)$$

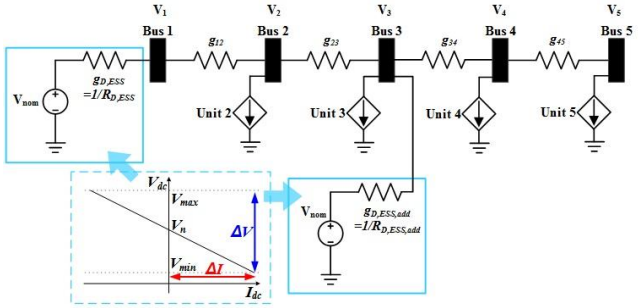

Fig. 10. Equivalent 5-bus DC MG with an ESS at bus-3

When the ESS is additionally placed on bus-3, the $g_{D,ESS,add}$ term is introduced in (18) and (A-3). Since [S] depends on the Jacobian matrix as shown in (12), it also depends on the bus where the DPS is additionally placed. That is, the voltage sensitivity [S] of the DC MG is dependent on the bus location where the DPS is placed. In this paper, a positioning method of the DPS is proposed to minimize the average voltage variation width Δv_{width} of the DC MG by independently analyzing [S] when a DPS is added to each bus.

By assuming that a DPS operated by droop control is added to bus-k in a DC MG with n-buses and that the power of bus-j fluctuates according to the rated capacity, the average voltage variation $\Delta v^{\pm}_{avg}$ and the average voltage variation width $\Delta v_{width,k}$ are defined as (19) and (20), respectively.

$$\Delta v^{\pm}_{avg,k} = \frac{1}{n}\sum_{i=1}^{n}\left(\pm\Delta v_{i,k}\right) = \frac{1}{n}\sum_{i=1}^{n}\sum_{j=1}^{n} s_{ij}\left(\pm\Delta p_{j,k}\right)\{i,\ \mathrm{j},\ \mathrm{k}\ \in \mathrm{n}\} \tag{19}$$

$$\Delta v_{width,k} = \Delta v^{+}_{avg,k} - \Delta v^{-}_{avg,k} \tag{20}$$

where $\Delta v_{i,k}$, $+\Delta p_{j,k}$, and $-\Delta p_{j,k}$ represent the voltage variation of bus-i, power consumption and generation at bus-j, respectively, when the DPS is additionally placed on bus-k.

Finally, the value of $\Delta v_{width,k}$ with various DPS positions can be calculated by using (20). Consequently, the proper bus location with the minimized $\Delta v_{width,k}$ can be determined.

Fig. 11 show the flowchart of the proposed positioning method. First, the position of DPS k, minimum average voltage variation width $\Delta v_{width,min}$, and proper bus location of DPS x are initialized. Next, the power equation of the DC MG when the DPS is located on the bus-k is derived through (9). Then, the voltage sensitivity $[S]_k$ is calculated by applying (10)-(12) and $\Delta v_{width,k}$ is calculated through (19)-(20). Finally, $\Delta v_{width,k}$ and $\Delta v_{width,min}$ is compared to find the value of $\Delta v_{width,min}$: when $\Delta v_{width,k}$ is smaller than $\Delta v_{width,min}$, $\Delta v_{width,k}$ is stored as $\Delta v_{width,min}$. Simultaneously, k is stored as x. Consequently, repeating the process by the total number of buses determines the final bus location that minimize $\Delta v_{width,k}$.

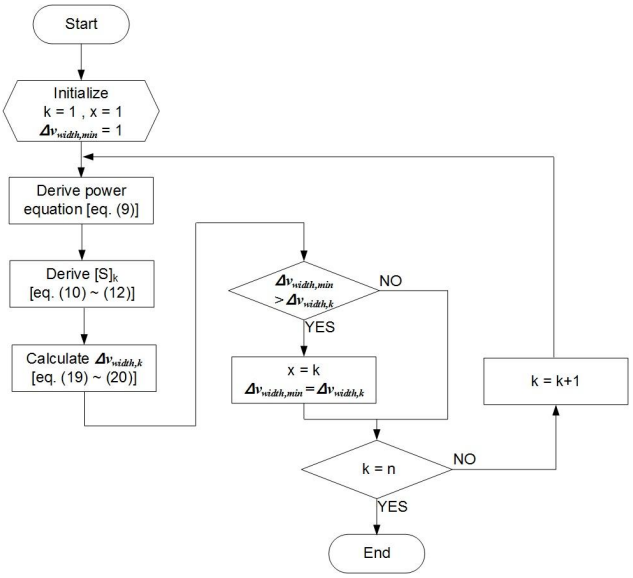

Fig. 11. Proposed positioning method

5. Case study

4 cases were simulated by PSCAD/EMTDC to validate the proposed positioning method. In case 1, the 5-bus DC MG shown in fig. 6 was simulated. In case 2 and 3, the structure of 5-bus DC MG of case 1 was changed to ring and mesh type, respectively. In case 4, a 13-bus DC MG was simulated.

In the all cases, it is assumed that a new ESS with the same rated capacity of the ESS on bus-1 is additionally placed and operated by droop control.

Case 1 is DC MG shown in fig. 6. Table 1 shows the location and rated capacity of each device. Table 2 shows the line constants.

Fig. 12 shows the output power and the bus voltage when the load placed on each bus increases simultaneously, in the case of the new ESS was placed on bus-4. As shown in fig. 12 (a), when loads $p_{2,load}$, $p_{3,load}$, $p_{4,load}$, and $p_{5,load}$ of buses -2, 3, 4, and 5 increase to the maximum rating at 0.1 s, the ESSs of bus-1 and bus-4 increase the output powers $p_{1,ESS}$ and $p_{4,ESS}$ to maintain the voltage of the DC MG. Due

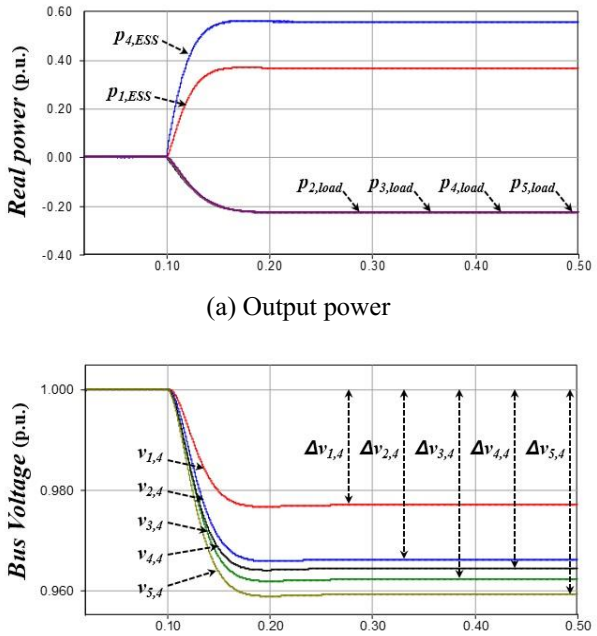

(a) Output power

(b) Bus voltage

Fig. 12. Output power and bus voltage variation of case 1; the new ESS is placed on bus-4

to the effects of the line impedance and the virtual impedance of droop control, these output power variations cause the voltage variation $\Delta v_{1\cdots5,4}$ that is shown in fig. 12 (b).

Fig. 13 shows the voltage of each bus when the new ESS is placed on bus-1 under the same conditions as those used in fig. 12. As can be seen from the figs. 12 and 13, the voltage variation of each bus depends on the location of the new ESS.

Fig. 14 shows the average voltage variation width $\Delta v_{sim,width,k}$ that was calculated by the simulation. $\Delta v_{sim,width,k}$ represents the minimum value $\Delta v_{sim,width,4}$ when an ESS is additionally located on bus-4.

Fig. 15 shows the average voltage variation width $\Delta v_{width,k}$ that was obtained numerically by using the proposed method. As shown in the figure, $\Delta v_{width,k}$ is the minimum at bus-4($\Delta v_{width,4}$) through the proposed positioning method. It means that bus-4 is the location where the new ESS can be added to produce the minimum voltage variation and indicates similar result in simulation.

Fig. 16 shows the error between the simulated results andthe results obtained by the proposed method. The maximum error is 0.00331 p.u., which is equal to about 4.9 *V*. In other words, the average voltage variation width $\Delta v_{width,k}$ of the DC MG that was predicted based on the voltage sensitivity is relatively accurate.

Fig. 17 shows the case 2, which is 5-bus DC MG with a ring structure. Compared to case 1, the line impedance $R_{25}(=1/G_{25})$ is added.

Fig. 18 shows the results of case 2. As shown in the figure, $\Delta v_{width,k}$ is the minimum at bus-4($\Delta v_{width,4}$) through

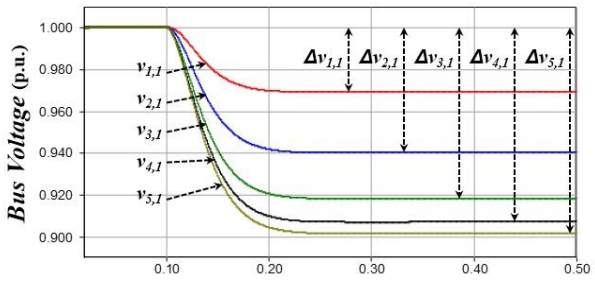

Fig. 13. Bus voltage variation of case 1; the new ESS is placed on bus 1

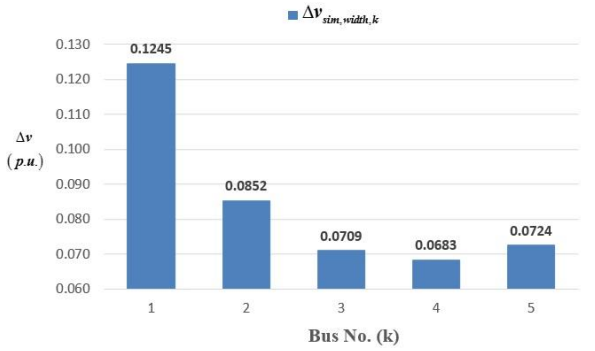

Fig. 14. Results of simulation in case 1

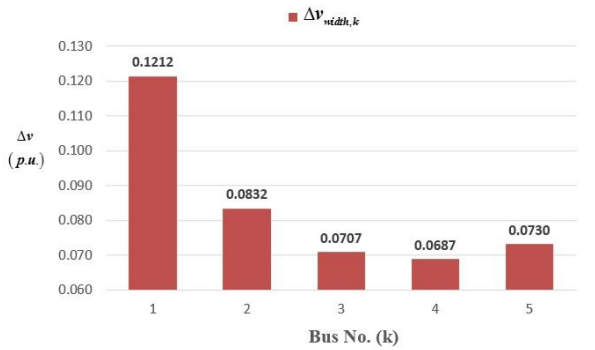

Fig. 15. Results of the proposed method in case 1

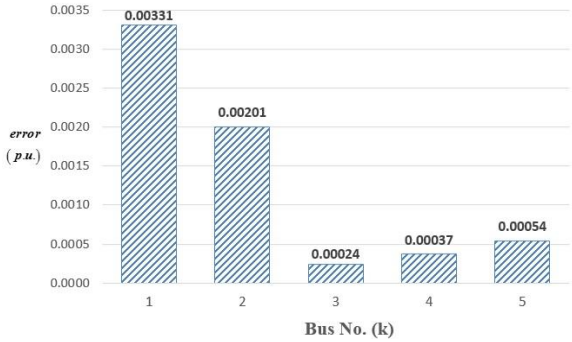

Fig. 16. Error between the results of case 1

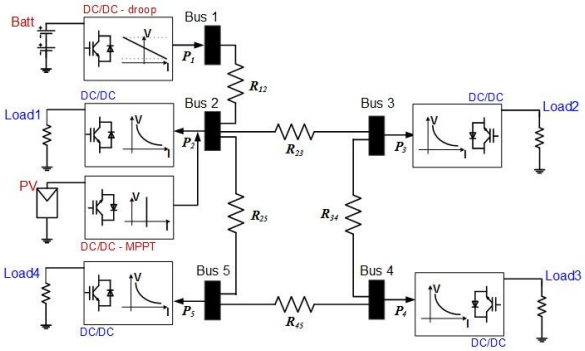

Fig. 17. Case 2 : Ring structure

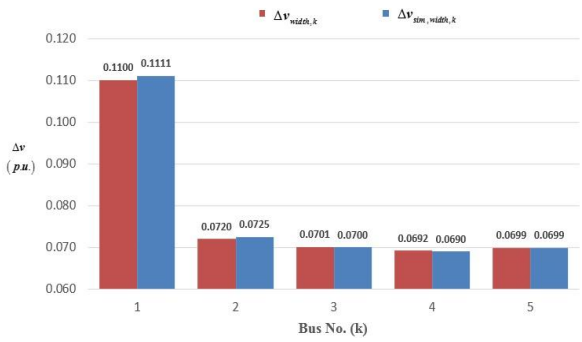

Fig. 18. Results of case 2

the proposed positioning method. Therefore, bus-4 is selected as the location of the new ESS. It indicates that bus-4 is where the new ESS should be placed to obtain the minimum average voltage variation. The simulation results also represent the minimum value $\Delta v_{sim,width,4}$ when the new ESS is located on bus-4. The maximum error between the simulated results and those obtained by the proposed method is 0.00103 p.u., which is about 1.54 *V*.

Fig. 19 shows the case 3, which is 5-bus DC MG with a mesh structure where the line impedance $R_{35}(=1/G_{35})$ is added to case 2.

Fig. 20 shows the results of case 3. As shown in the figure, $\Delta v_{width,k}$ is the minimum at bus-5($\Delta v_{width,5}$) through the proposed positioning method. Therefore, bus-5 is selected as the location of the new ESS. The simulation results also represent the minimum value $\Delta v_{sim,width,5}$ when

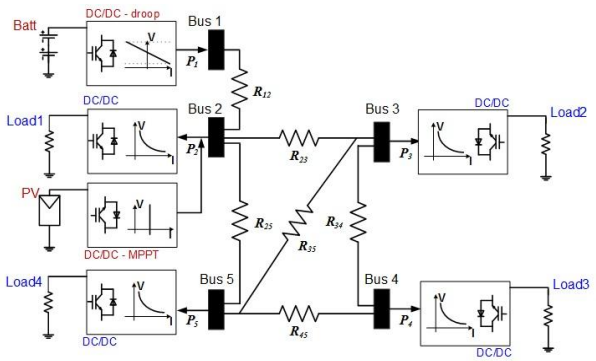

Fig. 19. Case 3 : Mesh structure

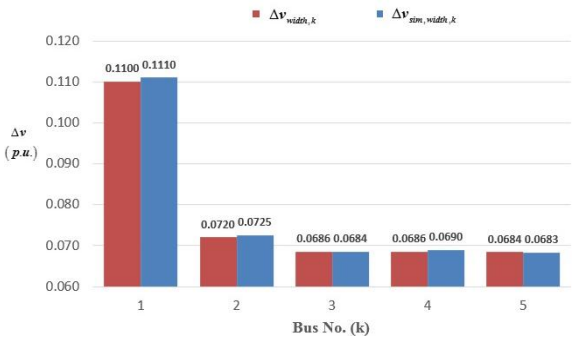

Fig. 20. Results of case 3

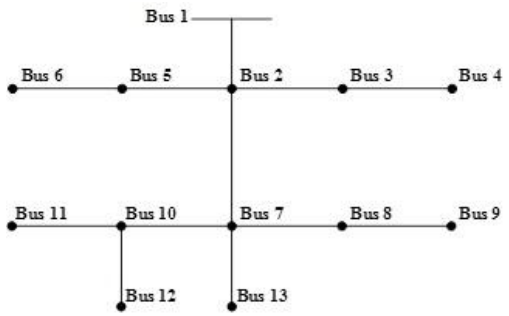

Fig. 21. Case 4 : 13-bus DCMG

the new ESS is located on bus-5. The maximum error is 0.00103 p.u.

Fig. 21 shows the case 4 which is the 13-bus DC MG. The system was constructed for case studies based on the IEEE 13-node test feeder system [17]. Table 3 and 4 lists the rated capacity for the 13-bus DC MG and the line resistance between buses, respectively. The nominal voltage, base power, and base impedance are the same as in the previous cases.

Table 5 shows the results of case 4. As shown in the table, $\Delta v_{width,k}$ is the minimum at bus-7($\Delta v_{width,7}$) through the proposed positioning method. Therefore, bus-7 is selected as the location of the new ESS. The simulation

Table 3. Rated power data for 13-bus DCMG

Bus No.	Units	Rating
1	ESS	110 kW
2	Load, PV	35 kW, 50 kW
3	Load	20 kW
4	Load	20 kW
5	Load	10 kW
6	Load	10 kW
7	Load, PV	15 kW, 40 kW
8	Load	30 kW
9	Load	10 kW
10	Load, PV	18 kW, 20 kW
11	Load	14 kW
12	Load	10 kW
13	Load	8 kW

Table 4. Resistance between bus for 13-bus DCMG

From Bus	To Bus	Resistance Ω
1	2	0.0294 Ω
2	3	0.0346 Ω
2	5	0.01358 Ω
2	7	0.06120 Ω
3	4	0.03951 Ω
5	6	0.02195 Ω
7	8	0.01730 Ω
7	10	0.04390 Ω
7	13	0.0173 Ω
8	9	0.03512 Ω
10	11	0.03073 Ω
10	12	0.03951 Ω

Table 5. Results of case 4

Symbol	Values	Symbol	Values
$\Delta v_{width,1}$	0.094349 p.u.	$\Delta v_{sim,width,1}$	0.097554 p.u.
$\Delta v_{width,2}$	0.091457 p.u.	$\Delta v_{sim,width,2}$	0.094457 p.u.
$\Delta v_{width,3}$	0.091984 p.u.	$\Delta v_{sim,width,3}$	0.094993 p.u.
$\Delta v_{width,4}$	0.092947 p.u.	$\Delta v_{sim,width,4}$	0.096010 p.u.
$\Delta v_{width,5}$	0.091727 p.u.	$\Delta v_{sim,width,5}$	0.094743 p.u.
$\Delta v_{width,6}$	0.092321 p.u.	$\Delta v_{sim,width,6}$	0.095379 p.u.
$\Delta v_{width,7}$	0.089048 p.u.	$\Delta v_{sim,width,7}$	0.091881 p.u.
$\Delta v_{width,8}$	0.089315 p.u.	$\Delta v_{sim,width,8}$	0.092152 p.u.
$\Delta v_{width,9}$	0.090263 p.u.	$\Delta v_{sim,width,9}$	0.093163 p.u.
$\Delta v_{width,10}$	0.089269 p.u.	$\Delta v_{sim,width,10}$	0.092116 p.u.
$\Delta v_{width,11}$	0.089719 p.u.	$\Delta v_{sim,width,11}$	0.092960 p.u.
$\Delta v_{width,12}$	0.090323 p.u.	$\Delta v_{sim,width,12}$	0.093240 p.u.
$\Delta v_{width,13}$	0.089901 p.u.	$\Delta v_{sim,width,13}$	0.092397 p.u.

results shows the minimum value $\Delta v_{sim,width,7}$ when the new ESS is located on bus-7. There is a uniform error which is about 0.003p.u., which is about 4.5V, between the calculation and the simulation results. It is a small error compared to the nominal voltage.

6. Conclusion

In this paper, a positioning method of a DPS that is operated by droop control is proposed. In order to improve the accuracy of the power flow analysis, a droop bus that considers the characteristics of droop control is introduced.

The dependency of the voltage sensitivity is also analyzed to find the proper bus location for the DPS. The proposed method is applied to various MG structures and the feasibility is verified through PSCAD/EMTDC simulation.

Acknowledgements

This research was supported by the KEPCO under the project entitled by "Demontration Study for Low Voltage Direct Current Distribution Network in an lsland (R15DA12)".

Appendix

$$[J]_{slack}=\begin{bmatrix} \begin{matrix}2v_2(g_{12}+g_{23})\\ -(g_{12}v_1+g_{23}v_3)\end{matrix} & -g_{23}v_2 & 0 & 0 \\ -g_{23}v_3 & \begin{matrix}2v_3(g_{23}+g_{34})\\ -(g_{23}v_2+g_{34}v_4)\end{matrix} & -g_{34}v_3 & 0 \\ 0 & -g_{34}v_4 & \begin{matrix}2v_4(g_{34}+g_{45})\\ -(g_{34}v_3+g_{45}v_5)\end{matrix} & -g_{45}v_4 \\ 0 & 0 & -g_{45}v_5 & 2g_{45}v_5-g_{45}v_4 \end{bmatrix} \tag{A-1}$$

$$[J]_{droop}=\begin{bmatrix} \begin{matrix}2v_1(g_{D,ESS}+g_{12})\\ -(g_{D,ESS}v_{nom}+g_{12}v_2)\end{matrix} & -g_{12}v_1 & 0 & 0 & 0 \\ -g_{12}v_2 & \begin{matrix}2v_2(g_{12}+g_{23})\\ -(g_{12}v_1+g_{23}v_3)\end{matrix} & -g_{23}v_2 & 0 & 0 \\ 0 & -g_{23}v_3 & \begin{matrix}2v_3(g_{23}+g_{34})\\ -(g_{23}v_2+g_{34}v_4)\end{matrix} & -g_{34}v_3 & 0 \\ 0 & 0 & -g_{34}v_4 & \begin{matrix}2v_4(g_{34}+g_{45})\\ -(g_{34}v_3+g_{45}v_5)\end{matrix} & -g_{45}v_4 \\ 0 & 0 & 0 & -g_{45}v_5 & 2g_{45}v_5-g_{45}v_4 \end{bmatrix} \tag{A-2}$$

$$[J]_{droop,bus3}=\begin{bmatrix} \begin{matrix}2v_1(g_{D,\mathrm{ESS}}+g_{12})\\ -(g_{D,ESS}v_{nom}+g_{12}v_2)\end{matrix} & -g_{12}v_1 & 0 & 0 & 0 \\ -g_{12}v_2 & \begin{matrix}2v_2(g_{12}+g_{23})\\ -(g_{12}v_1+g_{23}v_3)\end{matrix} & -g_{23}v_2 & 0 & 0 \\ 0 & -g_{23}v_3 & \begin{matrix}2v_3(g_{D,ESS,add}+g_{23}+g_{34})\\ -(g_{D,ESS,add}v_{nom}+g_{23}v_2+g_{34}v_4)\end{matrix} & -g_{34}v_3 & 0 \\ 0 & 0 & -g_{34}v_4 & \begin{matrix}2v_4(g_{34}+g_{45})\\ -(g_{34}v_3+g_{45}v_5)\end{matrix} & -g_{45}v_4 \\ 0 & 0 & 0 & -g_{45}v_5 & 2g_{45}v_5-g_{45}v_4 \end{bmatrix} \tag{A-3}$$

References

[1] R. H. Lasseter, "MicroGrids," in 2002 IEEE Power Engineering Society Winter Meeting. Conference Proceedings (Cat. No.02CH37309), vol. 1, pp. 305-308, 2002.

[2] J. M. Guerrero, J. C. Vasquez, J. Matas, L. G. d. Vicuna, and M. Castilla, "Hierarchical Control of Droop-Controlled AC and DC Microgrids;A General Approach Toward Standardization," *IEEE Trans. Industrial Electronics*, vol. 58, pp. 158-172, 2011.

[3] Y. Gu, X. Xiang, W. Li, and X. He, "Mode-Adaptive Decentralized Control for Renewable DC Microgrid With Enhanced Reliability and Flexibility," *IEEE Trans. Power Electronics*, vol. 29, pp. 5072-5080, 2014.

[4] T. Dragicevic, J. C. Vasquez, J. M. Guerrero, and D. Skrlec, "Advanced LVDC Electrical Power Architectures and Microgrids: A step toward a new generation of power distribution networks," *IEEE Electrification Magazine*, vol. 2, pp. 54-65, 2014.

[5] D. Salomonsson, L. Soder, and A. Sannino, "An Adaptive Control System for a DC Microgrid for Data Centers," *IEEE Trans. Industry Applications*, vol. 44, pp. 1910-1917, 2008.

[6] D. E. Olivares, C. A. Cañizares, and M. Kazerani, "A Centralized Energy Management System for Isolated Microgrids," *IEEE Trans. Smart Grid*, vol. 5, pp. 1864-1875, 2014.

[7] Y. Ito, Y. Zhongqing, and H. Akagi, "DC microgrid based distribution power generation system," *in The 4th International Power Electronics and Motion Control Conference*, 2004. *IPEMC* 2004., Vol. 3, pp. 1740-1745, 2004.

[8] S. Anand, B. G. Fernandes, and J. Guerrero, "Distributed Control to Ensure Proportional Load Sharing and Improve Voltage Regulation in Low-Voltage DC Microgrids," *IEEE Trans. Power Elec-tronics*, vol. 28, pp. 1900-1913, 2013.

[9] M. R. Vallem, J. Mitra, and S. B. Patra, "Distributed Generation Placement for Optimal Microgrid Architecture," *in 2005/2006 IEEE/PES Transmission and Distribution Conference and Exhibition*, pp. 1191-1195, 2006.

[10] N. Lin, B. Zhou, and X. Wang, "Optimal placement of distributed generators in micro-grid," *in 2011 International Conference on Consumer Electronics, Communications and Networks* (*CECNet*), pp. 4239-4242, 2011.

[11] A. K. Basu, A. Bhattacharya, S. P. Chowdhury, S. Chowdhury, and P. A. Crossley, "Reliability study of a micro grid system with optimal sizing and placement of DER," *in CIRED Seminar 2008: SmartGrids for Distribution,* pp. 1-4, 2008.

[12] C. Abbey and G. Joos, "Coordination of Distributed Storage with Wind Energy in a Rural Distribution System," *in 2007 IEEE Industry Applications Annual Meeting*, pp. 1087-1092, 2007.

[13] J. M. Gantz, S. M. Amin, and A. M. Giacomoni, "Optimal mix and placement of energy storage systems in power distribution networks for reduced outage costs," *in 2012 IEEE Energy Conversion Congress and Exposition (ECCE)*, pp. 2447-2453, 2012.

[14] Z. Chaorui and Z. Ying Jun, "Optimal distributed generation placement among interconnected cooperative microgrids," *in 2016 IEEE Power and Energy Society General Meeting (PESGM)*, pp. 1-5, 2016.

[15] Ali Keyhani, Design of Smart Power Grid Renewable Energy Systems, Wiley, 2011.

[16] C. Li, S. K. Chaudhary, M. Savaghebi, J. C. Vasquez, and J. M. Guerrero, "Power Flow Analysis for Low-voltage AC and DC Microgrids Considering Droop Control and Virtual Impedance," *IEEE Trans. Smart Grid*, vol. PP, pp. 1-1, 2016.

[17] H.-Y. Jeong, J.-C. Choi, D.-J. Won, S.-J. Ahn, and S.-i. Moon, "Formulation and Analysis of an Approximate Expression for Voltage Sensitivity in Radial DC Distribution Systems," Energies, vol. 8, pp. 9296,-9319, 2015.

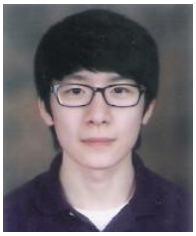

Byoung-Sun Ko He received B.S degree from Hanyang University, Ansan, Korea, in 2013. He is currently working toward the direct Ph.D. degree in the Department of Electrical Engineering, Hanyang University, Seoul, Korea. His current research interests include renewable energy system, control of microgrid, and grid-connected power converter.

Gi-Young Lee He received the B.S degree in electrical engineering from Hanyang University, Seoul, Korea, in 2013, where he is currently working toward the direct Ph.D. degree. His current research interests include modeling and control of distributed power converter systems, converters for renewable energies, and microgrids.

Sang-Il Kim He was born in Korea in 1975. He received the B.S., M.S. and the Ph.D degrees in electrical engineering from Hanyang University, Korea, in 1998, 2000 and 2017 respectively. From 2000 to 2005, he was a Researcher with POSCON Company, Korea. From 2005 to 2008, he was a

member of the research staff at Samsung Advanced Institute of Technology, Yongin, Korea. Since 2008, he has been a Chief Research Engineer at Doosan Robotics Company, Seoul, Korea. His current research interests are power electronics control of electric machines, sensorless drives, electric/hybrid vehicle, and power conversion circuits.

Rae-Young Kim received the B.S. and M.S. degrees from Hanyang University, Seoul, Korea, in 1997 and 1999, respectively, and the Ph.D. degree from Virginia Polytechnic Institute and State University, Blacksburg, VA, USA, in 2009, all in electrical engineering. From 1999 to 2004, he was a Senior Researcher at the Hyosung Heavy Industry R&D Center, Seoul, Korea. In 2009, he was a Postdoctoral Researcher at National Semiconductor Corporation, Santa Clara, CA, USA, involved in a smart home energy management system. In 2016, he was a Visiting Scholar with the Center for Power Electronics Systems (CPES), Virginia Polytechnic Institute and State University, Blacksburg. Since 2010, he has been with Hanyang University, where he is currently an Assistant Professor in the Department of Electrical and Biomedical Engineering. His research interests include modeling and control of distirbuted power converter systems, soft-switching techniques, energy management systems in microgrid applications, modular power converter for renewable energies and motor drive systems. Dr. Kim was a recipient of the 2007 First Prize Paper Award from the IEEE IAS.

Jin-Tae Cho He received the B.S. and M.S. degrees in electrical engineering from Korea University, Seoul, South Korea, in 2006 and 2008, respectively, where he is currently working toward the Ph.D. degree in dc distribution. He is currently a Senior Researcher at the Smart Power Distribution Laboratory, Korea Electric Power Corporation Research Institute, Daejeon, South Korea. His research interests include protection, monitoring, and control of LVdc distribution system.

Ju-Yong Kim He received the M.S. and Ph.D. degrees from Kyungpook National University, Daegu, South Korea, in 1994 and in 2007, respectively. In 1994, he joined the Korea Electric Power Corporation Research Institute, Daejon, South Korea, as a Researcher, where he is currently a Principal Researcher at the Smart Power Distribution Laboratory. His main research interests include dc distribution system and dc microgrid.